

Table I gives a comparison of the values of spontaneous polarization P_s and coercive field E_c of this family of ferroelectrics. Except for the case of (glycine)₂·MnCl₂·2H₂O, all of the values of P_s and E_c are taken at temperatures about 10° below the respective Curie points. No Curie temperature is observable for (glycine)₂·MnCl₂·2H₂O and the P_s and E_c values for it are those at room temperature.⁴

VI. ACKNOWLEDGMENTS

This research is supported by contracts with the Army Signal Corps Engineering Laboratories and the Air Force Office of Scientific Research. We are grateful to Dr. S. Triebwasser of the IBM Research Laboratory in Poughkeepsie, New York, for discussions, to Mrs. Ann Diamond for assistance in crystal growth, and to Miss Bertha Scubon for preliminary dielectric measurements.

Radiation Damage in Ge and Si Detected by Carrier Lifetime Changes: Damage Thresholds*

J. J. LOFERSKI AND P. RAPPAPORT
RCA Laboratories, Princeton, New Jersey
(Received March 11, 1958)

Minority carrier lifetime, τ , in semiconductors is shown to be more sensitive, by a factor of 10⁴, to radiation-induced defects than the conductivity. Thus, in some cases, the introduction of as few as 10¹⁰ defects per cm³ can be detected by its effect on τ . Both direct measurements of τ , and measurements of dependent parameters (such as the photovoltaic effect and the particle voltaic effect) are described for Si and Ge. Using such parameters, and an electron accelerator, the minimum energy needed to produce a Frenkel defect was found to be 14.5±0.4 eV in Ge and 12.9±0.6 eV in Si. An analysis of the phenomenon shows how the location of the radiation-induced energy levels and the relative minority carrier capture cross sections can be determined experimentally. The shape of the curve of the displacement cross section *versus* the incident particle energy is compared to calculations from collision theory. Qualitative explanations for the observed "tail" on this curve are presented. Calculations based on these explanations fail to yield complete agreement with the experimental curves.

LIST OF IMPORTANT SYMBOLS

σ ≡ conductivity of semiconductor.
 τ ≡ minority carrier bulk lifetime.
 N_r ≡ density of recombination centers.
 σ_c ≡ cross section for minority carrier capture.
 v ≡ thermal velocity of carriers.
 $\Delta(E_B)$ ≡ cross section for Frenkel defect formation.
 ρ ≡ resistivity of semiconductor.
 N_B ≡ number of bombarding particles per unit time.
 ϕ ≡ integrated bombarding flux.
 t ≡ time of bombardment.
 I_B ≡ current of bombarding particles.
 E_B ≡ energy of bombarding particle.
 E_{B0} ≡ minimum energy of impinging particles for producing defects.
 E_L ≡ energy imparted to a lattice atom in a collision.
 E_i ≡ energy level of recombination center.
 E_f ≡ energy of Fermi level.
 I_s ≡ photovoltaic short circuit current.
 e ≡ electron charge.
 L ≡ diffusion length of minority carriers.

g ≡ electron-hole pair generation rate.
 D ≡ diffusion constant for minority carriers.
 Q ≡ fraction of generated carriers collected by a junction.
 α ≡ absorption constant for light.
 s ≡ surface recombination velocity.
 l ≡ semiconductor thickness.

I. INTRODUCTION

THE simplest consequence of a collision between a particle of high kinetic energy and an atom in a solid is the displacement of the struck atom to an interstitial position. By definition, the resulting vacancy-interstitial pair constitutes a Frenkel defect. Such defects can be introduced into the lattice only if the energy transferred to the crystal atom by the impinging particle is equal to, or exceeds, a threshold energy, which is identified with the energy that constrains the atom to remain in its equilibrium position. The magnitude of this threshold energy is of fundamental importance to an understanding of the mechanism of radiation damage and of crystal forces. Of the parameters available for measurement in previous experiments, the electrical conductivity, σ , seemed to be most sensitive to the presence of Frenkel defects. Consequently,

* Preliminary reports of this work have been given in earlier brief communications; *viz.*, P. Rappaport, Phys. Rev. **94**, 1409(A) (1954); J. J. Loferski and P. Rappaport, Phys. Rev. **98**, 1861 (1955); and P. Rappaport and J. J. Loferski, Phys. Rev. **100**, 1261(A) (1955).

the thresholds of Cu,¹ Fe,² and Ge³ were determined by establishing the minimum energy a bombarding electron must have in order to produce a detectable change in σ . This paper describes experiments which used a much more sensitive parameter than σ , namely, τ , the lifetime of minority carriers in a semiconductor, to detect the presence of Frenkel defects and, therefore, to determine the threshold for production of such defects. The sensitivity of τ to the presence of energy levels near the center of the forbidden energy gap has been shown theoretically by Hall,⁴ and Shockley and Read,⁵ and demonstrated experimentally for certain chemical impurities by Burton *et al.*⁶ These investigators concluded that concentrations of such levels in the range of $10^{12}/\text{cc}$ determine τ . The conductivity, on the other hand, depends on concentrations of about 10^{15} levels/cc. That bombardment-induced Frenkel defects do in fact introduce levels near the center of the gap has already been shown.^{7,8}

II. BASIC CONCEPTS

(a) Relation Between τ and Irradiation Time

The relation between τ and the density of recombination centers, N_r , is given by^{4,5}

$$1/\tau = N_r \sigma_c v f(E_t - E_f), \quad (1)$$

where σ_c is the minority carrier capture cross section, v is the thermal velocity of the carriers, and $f(E_t - E_f)$ is a function of the location of the recombination centers, E_t , with respect to the Fermi level, E_f , which reduces to unity for heavily doped *p*- or *n*-type material, but is a sensitive function of ρ if E_f is close to E_t .

Furthermore, if more than one species of recombination centers exist, it is presumed that there is no interaction and that

$$1/\tau = \sum_i (1/\tau_i) = \sum_i N_{ri} \sigma_{ci} v f(E_{ti} - E_f). \quad (2)$$

For the low flux levels employed in these experiments, it is reasonable to assume that the number of recombination centers introduced is proportional to the flux bombardment time product $N_B t$, i.e., the integrated flux, ϕ , and to the cross section for defect formation, $\Delta(E_B)$. Thus it follows that

$$N_{rB} = N_B \Delta(E_B) t = \Delta(E_B) \phi, \quad (3)$$

and

$$1/\tau = 1/\tau_0 + N_B \Delta(E_B) \sigma_c v f_B(E_{tB} - E_f) t, \quad (4)$$

¹ D. T. Eggen and M. J. Laubenstein, Phys. Rev. **91**, 238(A) (1953).

² J. M. Denney, Phys. Rev. **92**, 531(A) (1953).

³ E. E. Klontz and K. Lark-Horovitz, Phys. Rev. **86**, 643(A) (1952). See also E. E. Klontz, thesis, Purdue University, 1952 (unpublished).

⁴ R. N. Hall, Phys. Rev. **87**, 387 (1952).

⁵ W. Shockley and W. T. Read, Phys. Rev. **87**, 835 (1952).

⁶ Burton, Hull, Morin, and Severiens, J. Phys. Chem. **57**, 853 (1953).

⁷ H. M. James and K. Lark-Horovitz, Z. Physik, Chem. **198**, 107 (1951).

⁸ Cleland, Crawford, and Pigg, Phys. Rev. **98**, 1742 (1955); **99**, 1170 (1955).

where the subscript *B* refers to parameters associated with bombardment-produced defects. Equation (4) predicts a linear relation between τ^{-1} and t if N_B is constant, with a slope given by

$$d(\tau^{-1})/dt = N_B \Delta(E_B) \sigma_c v f_B. \quad (5)$$

From such plots the following information is obtained:

(a) If E_B alone is varied, it is possible to determine how the cross section for defect formation varies with bombardment energy. The shape of this curve can then be compared to that of the theoretically calculated cross-section curve. From such a comparison one can infer whether theory and experiment are based on the same mechanism for defect formation. As a corollary to the $\Delta(E_B)$ vs E_B curve, the threshold energy, E_{L0} , which must be transferred to a host lattice atom in order to displace it from its normal position, can be determined by observing the value of E_B for which $\Delta(E_B)$ vanishes. Any variation of the thresholds with temperature, crystal orientation, dislocation density, etc. can also be established.

(b) If samples of different resistivities are exposed to the same source, i.e., $N_B \Delta(E_B)$ is constant, one can plot f_B vs E_f and compare with theory. Such a comparison can demonstrate whether the bombardment-induced recombination centers are characterized by a single energy level, E_t , or by multiple levels. If a single level is indicated, its location can be calculated from the experimental curve. Since f_B becomes unity in heavily doped *p*-type or *n*-type material, comparing rates of decay in the two material types allows the ratio of cross sections for capture of carriers to be determined. If, furthermore, the absolute value of $\Delta(E_B)$ is known, the actual cross sections, σ_{cn} and σ_{cp} , can be deduced.

(b) Parameters Related to τ

Because experimental difficulties are encountered in a direct measurement of τ , it is advantageous to use more easily measured parameters which bear a simple relation to τ . Three such parameters have suggested themselves thus far, namely: (i) the short circuit current, I_s , of the photovoltaic effect or of the voltaic effect accompanying α , β , and γ rays or any other ionizing radiation; (ii) the collector to base amplification factor, α_{cb} , of a transistor,⁹ and (iii) the radiation emitted because of the recombination of excess minority carriers injected into a semiconductor.¹⁰ Both I_s and the recombination radiation share the advantage that they permit observation of bombardment-induced recombination centers in materials whose τ is too low to be measured by conventional means, i.e., $\tau < 10^{-7}$ sec. It has been estimated that these parameters could follow changes in τ down to values of 10^{-10} sec. The experimental work described in this paper exploited the relation between I_s and τ . Many of the conclusions con-

⁹ J. J. Loferski, J. Appl. Phys. **29**, 35 (1958).

¹⁰ R. Braunstein, Bull. Am. Phys. Soc. Ser. II, **2**, 157 (1957).

cerning the utilization of I_s can, however, be applied to the other two parameters.

(c) Dependence of I_s on τ

Observation of I_s requires a p - n junction in the semiconductor. When ionizing radiation generates excess minority carriers near such a junction, some of them will diffuse to the junction and appear as a current in an external load resistance, R_L . Measurements of I_s are made with values of R_L which effectively short circuit the junction.¹¹ If the ionizing radiation injects carriers uniformly throughout the semiconductor and there are no losses due to recombination at the surface, all the minority carriers within a diffusion length, L , of the junction will be collected and

$$I_s = egL, \quad (6)$$

where I_s is the short-circuit current for unit area of junction, e is the electronic charge, and g is the generation rate of minority carriers produced by the radiation. Now

$$L^2 = D\tau, \quad (7)$$

where D is the diffusion constant for minority carriers. Therefore

$$I_s^2 = (eg)^2 D\tau. \quad (8)$$

In actual experiments, departures from this ideal case are encountered. The injection is not uniform and there are losses due to surface recombination so that only a fraction, Q , of the injected carriers appear in the measured I_s , i.e.,

$$I_s = Qeg. \quad (9)$$

The functional dependence of Q on the absorption

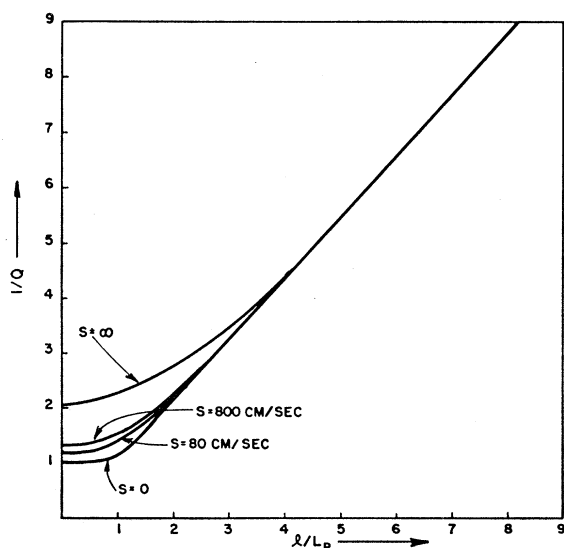


FIG. 1. A plot of the collection efficiency, Q , vs l/L_p for various values of s . ($l = 1/80$ cm, $\alpha = 8$).

¹¹ Rappaport, Loferski, and Linder, RCA Rev. 17, 100 (1956).

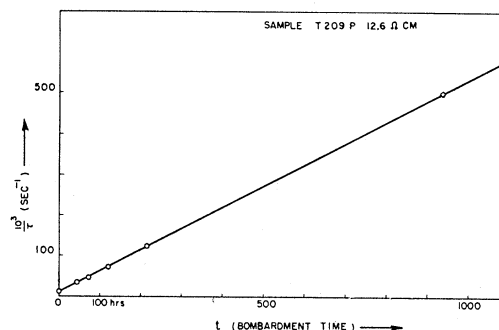


FIG. 2. Plots of τ vs t for an n -type Ge sample.

constant of the radiation, α , the surface recombination velocity, s , the thickness of the semiconductor, l , and the bulk lifetime, τ , has been calculated for the simple plane geometry used in our experiments.¹² In Fig. 1, we have plotted Q^{-1} vs L^{-1} for the values of s , indicated. Note that Q , and therefore I_s , remains proportional to L as L decreases, except for small values of l/L_p .

(d) Source of I_s

Three different relations between the ionizing radiation producing I_s and the damage-producing radiation have been explored:

(i) Ionization and damage can be produced by the same radiation. Thus α and β particles and γ rays will produce voltaic effects, whose I_s can be used to monitor the effect of the defects introduced by the same radiation. Most of our work with high-energy electrons falls into this category.

(ii) An ionizing radiation producing negligible damage may be present as a natural companion of a damaging radiation. For example there is a γ background associated with the neutrons in a reactor and the γ -voltaic effect can be used to monitor the neutron-produced damage.

(iii) An independent source of ionization can be supplied. Thus an intense light will produce a strong photovoltaic I_s whose variation during irradiation by damaging particles can be observed. This technique provides the highest possible sensitivity since I_s caused by light can be made to exceed by orders of magnitude the I_s caused by γ rays, α or β particles, or other ionizing radiation. Furthermore, a photovoltaic effect can usually be observed in materials which shows only a weak β - or γ -voltaic effect.

III. DESCRIPTION OF THE EXPERIMENTS

In these experiments the effect of β irradiation on τ was inferred from direct measurement of τ as well as from measurements of I_s .

¹² Rappaport, Loferski, and Linder, RCA Rev. 17, 125 (1956).

(a) Direct Measurement of τ

Samples of germanium 0.5 mm×4.0 mm×7.0 mm with various values of initial lifetime and initial resistivity were irradiated by β particles from a $\text{Sr}^{90}\text{-Y}^{90}$ source having a nominal activity of 50 mC. The spectrum of particles emitted by the source has been described elsewhere.¹¹ The average energy, E_B , of the emitted particles was about 1.0 Mev and the maximum energy, $E_{B \text{ max}}$, was 2.2 Mev. The half-life of the source (25 years) is conveniently long. An electron of average energy has a range of 0.75 mm in Ge, and 1.5 mm in Si. Although the defects are not distributed uniformly in the sample, there will be some throughout the volume.

To insure that the true bulk lifetime, independent of surface effects, would be measured in the 0.5 mm thick samples, τ was first determined for three samples of 2.0-mm, 1.0-mm, and 0.5-mm thicknesses. The apparatus used for these measurements is described elsewhere.¹³ The samples were etched in No. 5 etch which produces a surface having a low surface recombination velocity s of about 50 cm/sec.¹⁴ The observed τ was the same for the three thicknesses of a given set, showing that measurements on the 0.5 mm thick samples used for bombardment would yield surface-independent values of τ . After each bombardment, the units including the unirradiated controls in each set were re-etched and τ was measured. Such procedure insured that the value of s before and after bombardment was the same. Similar tests were performed for all the resistivities used.

The observed changes in τ during bombardment were very large, i.e., an order of magnitude in one hour for n -type samples of low ρ . Figure 2 shows a plot of $1/\tau$ vs t for 1000 hr. The linearity between $1/\tau$ and t indicates that the behavior of τ is as predicted by Eq. (4). From observations of changes in σ during bombardment, Klontz³ has shown that the probability that a 1-Mev electron will introduce a defect/cc is between

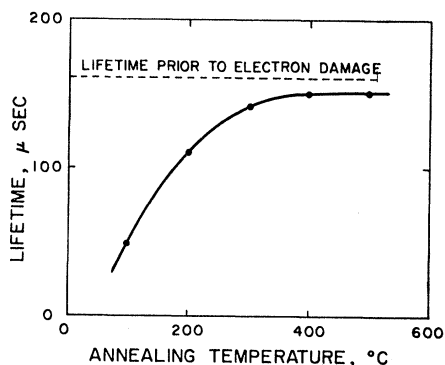


FIG. 3. Annealing of τ . The points on the curve show the value of τ after two hours baking at the indicated temperatures.

¹³ D. T. Stevenson and R. J. Keyes, J. Appl. Phys. 26, 140 (1955).

¹⁴ S. G. Ellis, J. Appl. Phys. 28, 1262 (1957).

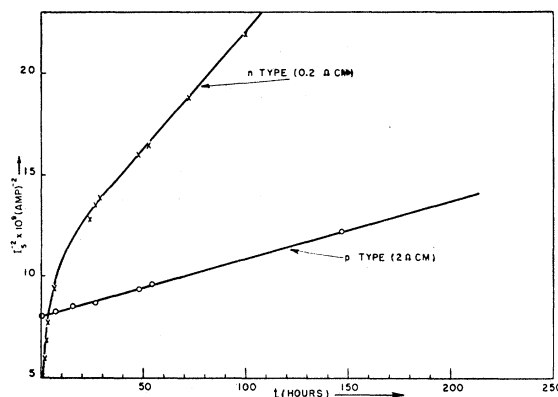


FIG. 4. Plots of I_s^{-2} vs t for a low ρ n -type and a low ρ p -type sample.

0.1 and 0.01. If one assumes that the same defects affect σ and τ , then one finds that after one hour of bombardment N_τ , as given by Eq. (3), is about $10^{11}/\text{cc}$ and σ_c , as computed from Eq. (5) and the slopes of $1/\tau$ vs t plots of Fig. 2, is about $5 \times 10^{-14} \text{ cm}^2$ for minority holes and $3 \times 10^{-16} \text{ cm}^2$ for minority electrons. These values are of the same order of magnitude as minority carrier capture cross sections reported for Ni and Cu recombination centers in Ge.⁶ The increased sensitivity for detection of defects which is permitted by observations of τ is evident, since 10^{11} defects/cc can change τ by an order of magnitude, whereas about 10^{14} defects are needed to produce a much smaller change in σ .

(b) Annealing of Recombination Centers

Irradiation-induced changes in τ do not anneal out appreciably at room temperature. Preliminary studies of the effect of annealing at elevated temperatures on the germanium lifetime samples were studied by F. D. Rosi of these Laboratories. His results are shown in Fig. 3. Here it is seen that for annealing times of two hours the original lifetime is almost recovered at temperature above 400°C , and that at room temperature there is little recovery, as stated.

(c) Measurement of I_s

The source of I_s was the voltaic effect produced by bombarding p - n junctions with β particles. A potentiometer was used to measure I_s , which for a typical Ge sample bombarded by the aforesaid $\text{Sr}^{90}\text{-Y}^{90}$ source, had a value of about $20 \mu\text{a}$. In this setup it was possible to follow changes in I_s for about three orders of magnitude to an accuracy better than $\pm 10\%$.

Equation (8) predicts that plots of I_s^{-2} vs t will be linear if Eq. (4) holds. Figure 4, in which I_s^{-2} is plotted vs t for a diode sample with an n -type base and for another with a p -type base, shows that except for the initial part of the curve of the n -type unit, such is indeed the case. The initial part of the curve has been attributed to a change in surface recombination velocity,

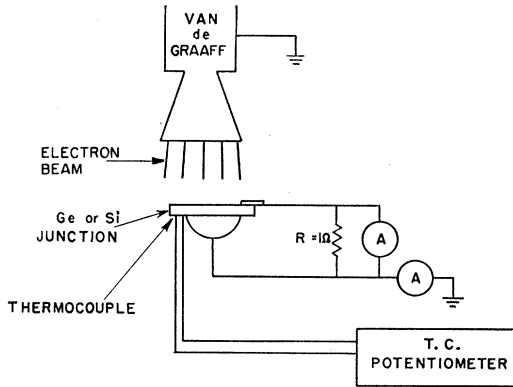


FIG. 5. Experimental arrangement for threshold experiments.

and the subsequent linear portion of the curve, which persists to the longest bombardment time used (300 hr), is identified with the relation predicted in Eq. (4). If one compares the slopes of plots like those of Fig. 4 with slopes of τ^{-1} vs t for the same initial τ , one finds that the slopes are related by the constants of Eq. (8).

(d) Measurement of Thresholds for Radiation Damage

Because of the demonstrated correlation between changes in τ and those in I_s , and because of the ease of measuring the latter, observation of the I_s of the voltaic effect caused by high-energy electron bombard-

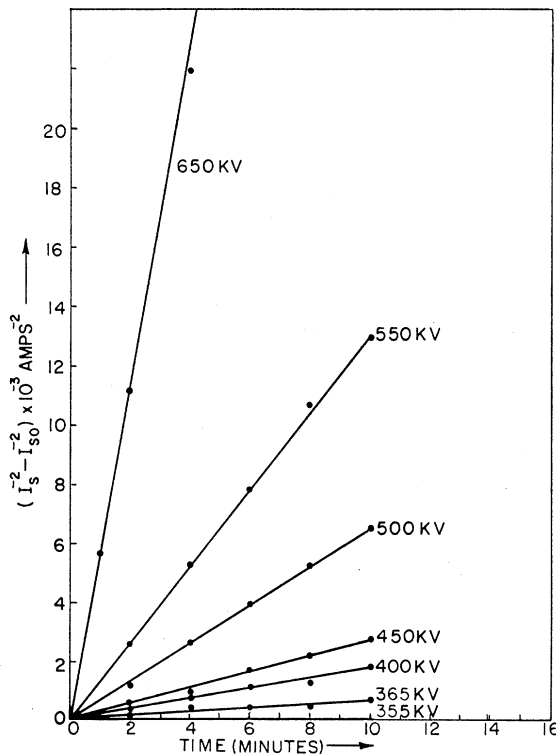


FIG. 6. Plots of $(I_s^{-2} - I_{s0}^{-2})$ vs t for Ge.

ment was used to determine thresholds for the onset of radiation damage, and the shape of the $\Delta(E_B)$ vs E_B curve for both Ge and Si. A 2-Mv Type AD-2 Van de Graaff generator, which supplied electrons at a fixed energy and a constant flux rate, was used for this study.¹⁵ Since Klontz³ had previously shown for Ge that changes in σ would occur only if the energy of the bombarding electrons exceeded a threshold of 630 kev, the effect on τ of electrons in the vicinity of this threshold was therefore examined.

A schematic of the experimental setup is shown in Fig. 5. Alloy type $p-n$ junctions on Ge and Si were bombarded on the side opposite the alloy dot. The wafers were about 0.008 in. thick, the alloy dots were 0.25 in. in diameter and the penetration depth of the alloy front was about 0.001 in. The base wafers had a resistivity of 0.5 ohm cm, n type, for Ge, and 30 ohm cm, p type, for Si. The alloy dot materials were In on Ge and an Au-Sb eutectic alloy on Si. The diodes were mounted in a water-cooled Cu block, whose temperature, as monitored by a thermocouple attached to a "dummy" sample, remained constant at 16°C. The samples were exposed to the atmosphere of the room.

The bombarding electrons were admitted into the air of the room after passing through a 0.003-in. Al

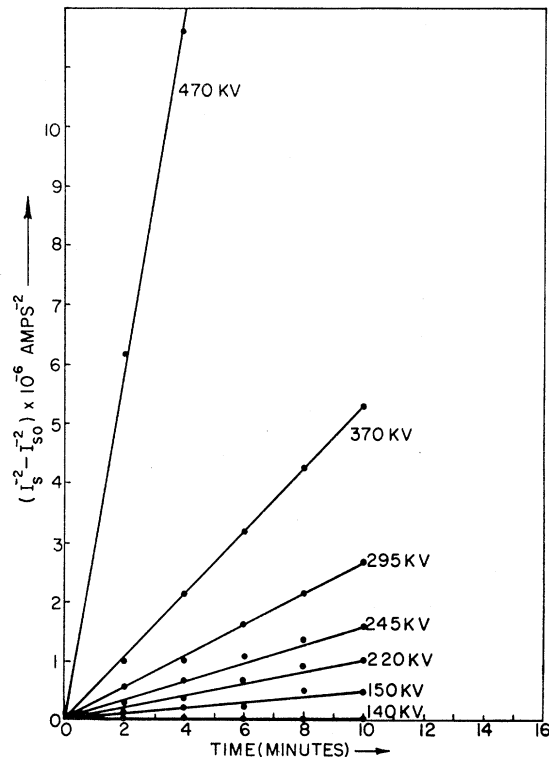


FIG. 7. Plots of $(I_s^{-2} - I_{s0}^{-2})$ vs t for Si.

¹⁵ This work was done at the High Voltage Engineering Corporation in Cambridge, Massachusetts. The authors wish to thank Mr. A. John Gale, who supervised the adaptation of the machine for these experiments and its calibration by means of the $\text{Be}^9(\gamma, n)$ reaction at 1.63 Mev.

window for Ge and a 0.001-in. Al window for Si. The energy of the electrons incident on the sample has been corrected for losses in the window and the air in front of the sample, and in what follows, E_B is the corrected maximum energy of the incident electrons. These corrections were calculated from the data of White and Millington,¹⁶ and result in a reduction of $E_{B \text{ max}}$ by 0.79 kev/mg cm² equivalent absorber thickness.

The accelerating voltage for the electrons was kept constant to within less than 1% while the current, as measured by either a Faraday cup or an insulated Ge or Si wafer in the plane of the bombarded samples, did not vary more than about 5%. (I_B was usually measured by using a semiconductor wafer whose thickness was the same as that of the bombarded diodes, so that the current absorbed in the samples, rather than that incident thereon, was the observed parameter.) The threshold experiments were performed by increasing E_B in 10-kev steps near the threshold and in 50-kev steps at higher energies, while the current absorbed in the bombarded region, whose area was 0.30 cm², was kept constant at 10⁻⁷ amp. Four samples were bombarded simultaneously.

As before, I_s of the electron voltaic effect was monitored with a potentiometer by shunting the diode with a 1-ohm resistor. Figure 6 shows the plot of I_s^{-2} vs t

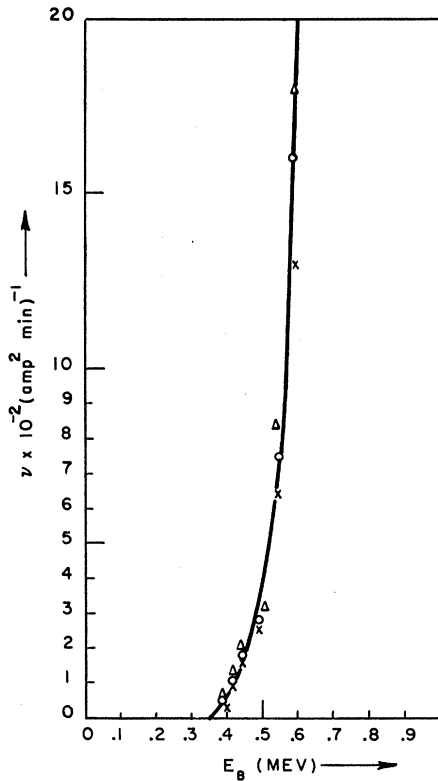


FIG. 8. Plots of $\nu[d(I_s)^{-2}/dt]$ vs E_B for Ge.

¹⁶ P. White and G. Millington, Proc. Roy. Soc. (London) A120, 701 (1928).

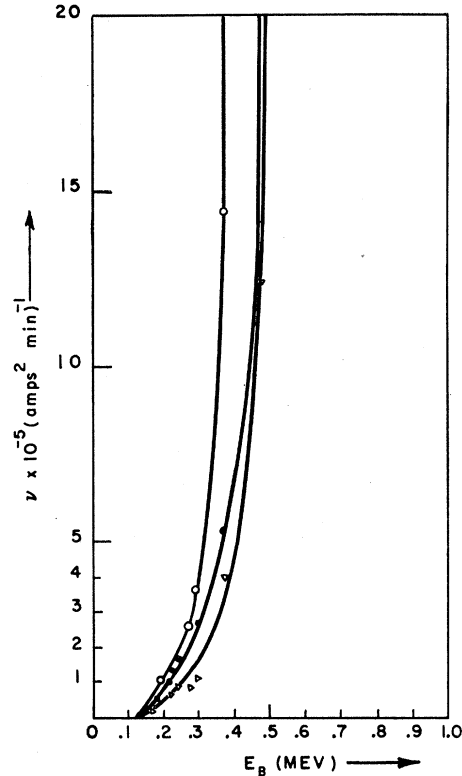


FIG. 9. Plots of ν vs E_B for Si.

for four Ge diodes at energies from 355 kev to 650 kev. Note again, that the relation between I_s^{-2} and t is linear as predicted by Eqs. (4) and (8). The slopes of successive curves, which according to Eq. (4) should be proportional to $\Delta(E_B)$, increase with E_B . Of special significance is the absence of a change in I_s in Ge for $E_B=355$ kev. A similar set of data is shown in Fig. 7 for Si. Note here the absence of a change in I_s for $E_B=140$ kev.

Figures 8 and 9 show the values of $dI_s^{-2}/dt[\equiv \nu(E_B)]$ vs E_B for the lines of Figs. 6 and 7. The data of Fig. 8 are an average for three Ge samples. From this curve it is concluded that $\Delta(E_B)=0$ for an electron energy between 355 kev and 365 kev. We have arbitrarily assumed that E_{L0} is halfway between these values, or 360 ± 5 kev. This corresponds to 14.5 ± 0.4 ev imparted to the Ge atom, to produce detectable changes in I_s .

Figure 9 is a similar plot for three separate silicon $p-n$ junctions. The lack of consistency in values of ν for the three samples has been traced to the existence of an appreciable contact series resistance which prevented measurement of the true junction short-circuit current. While this problem reduces the significance of the shape of the $\nu(E_B)$ vs E_B curve for Si, it does not affect the threshold energy which lies between 140 kev and 150 kev. As with Ge, we assume that E_{L0} is halfway between at 145 kev, which corresponds to 12.9 ± 0.6 ev imparted to a Si atom.

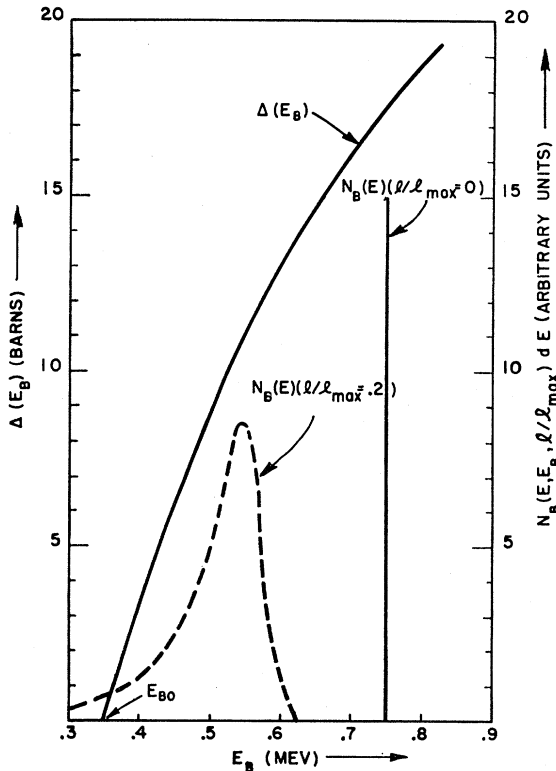


FIG. 10. Probability of displacing an atom, $\Delta(E_B)$ vs incident electron energy, E_B . Also the electron distribution function for an initially monoenergetic line after it has passed through a finite absorber thickness.

IV. DISCUSSION OF THRESHOLD RESULTS

(a) Threshold Value

The value of E_{L0} for Ge given above (14.5 eV) is lower than that found by Klontz (31 eV)⁸ and Vavilov *et al.* (22 eV)¹⁷ from observations of changes in σ . It is however in reasonable agreement with experiments on σ changes of Brown and Augustyniak¹⁸ (~14 eV). This latter value and that reported in this paper agree with the calculation of Kohn,¹⁹ who concluded that E_{L0} for Ge should lie between 7 eV and 15 eV.

No other determination of E_{L0} in Si has been reported. It is not surprising that its value (12.9 eV) lies so close to that of Ge, since both elements have similar lattice structures.

(b) Shape of $\Delta(E_B)$ vs E_B Curves

If one assumes Rutherford scattering of the electrons by the atoms in a crystal, the calculated cross section, $\Delta(E_B)$, for displacing an atom depends on the initial

energy of the (monoenergetic) electrons, E_B , as shown in Fig. 10, where the curve is computed for Ge with $E_{B0}=360$ kev.²⁰ One would expect that the shape of this curve should resemble that of the $\nu(E_B)$ versus E_B curves of Figs. 8 and 9. The latter, however, have "tails" rather than the sharp cutoff of Fig. 10. A number of reasons for this difference have been considered as follows:

(i) The sample has a finite thickness so that the initially monoenergetic electron beam develops a dispersion in velocity as a result of scattering, as shown by the dashed curve in Fig. 10. In this figure the initially monoenergetic line which impinges on the surface is shown beside a plot of $N_B(E, l/l_{max}, E_B)dE$, versus E_B , where $N_B(E, l/l_{max}, E_B)$ is the number of electrons whose energy lies between E and $E+dE$ after the beam has traversed a thickness l of the sample, and the thickness needed to stop the electrons is l_{max} . For the shape of this curve we used the experimental results of White and Millington.¹⁶ The dispersion is taken into account by computing the integral

$$\Delta(E_B, l/l_{max}) = \frac{1}{\langle N_B \rangle} \int_{E_{B0}}^{E_B} N_B(E, l/l_{max}, E_B) \Delta(E) dE \quad (10)$$

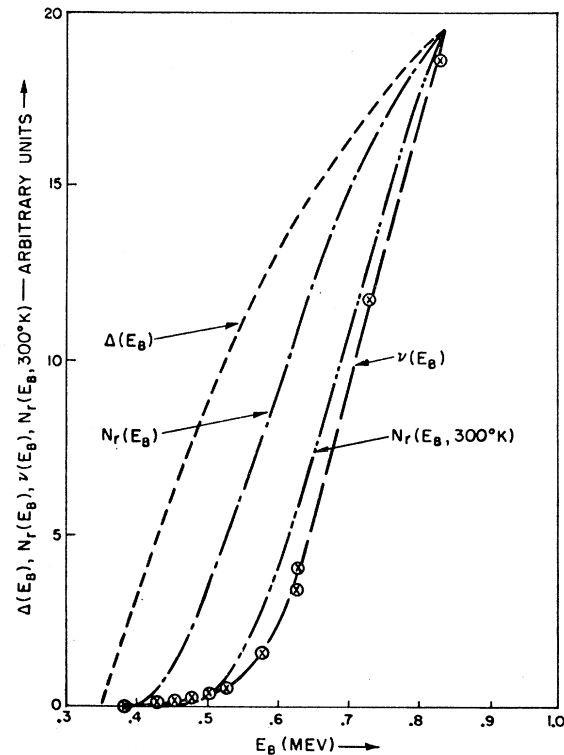


FIG. 11. The number of recombination centers, $N_r(E_B)$ vs E_B calculated at 0°K and at 300°K compared to $\Delta(E_B)$ and to experimentally observed $\nu(E_B)$.

¹⁷ Vavilov, Smirnov, Galkin, Spitsyn, and Patskevich, J. Tech. Phys. U.S.S.R. 26, 1865 (1956) [translation: Soviet Phys. (Tech. Phys.) 1, 1805 (1957)].

¹⁸ W. L. Brown and W. M. Augustyniak, Bull. Am. Phys. Soc. Ser. II, 2, 156 (1957).

¹⁹ W. Kohn, Phys. Rev. 94, 1409(A) (1954).

²⁰ See for example F. Seitz and J. S. Koehler, in *Solid State Physics*, edited by F. Seitz and D. Turnbull (Academic Press, Inc., New York, 1956), Vol. 2, p. 331.

for each of ten values of l/l_{\max} . Here E_B is the initial energy of the bombarding electrons, E_{B0} is the threshold energy, and $\langle N_B \rangle$ is the incident electron flux. The total number of recombination centers, $N_r(E_B)$, was then found from the expression

$$N_r(E_B) = N_A \langle N_B \rangle \int_0^{l=\lambda} \Delta(E_B, l/l_{\max}) dl, \quad (11)$$

where N_A is the number of atoms per cc, and λ is l_{\max} or the sample thickness, l , whichever is smaller. An additional assumption used in the calculation is that for monoenergetic electrons

$$\int_0^{E_B} N_B(E, l/l_{\max}, E_B) dE = (1 - l/l_{\max}) \langle N_B \rangle. \quad (12)$$

The results of such a calculation for Ge are shown in Fig. 11 which shows $\Delta(E_B)$, $N_r(E_B)$, and $\nu(E_B)$ vs E_B . The curves were normalized by assuming that they converged for energies in the vicinity of 1 Mev, and arbitrary units were used for these parameters. It is evident that $N_r(E_B)$ resembles $\nu(E_B)$ in lacking a sharp cutoff, so that at least part of the "tail" in the $\nu(E_B)$ vs E_B curve can be attributed to the dispersion. However, $\nu(E_B)$ has a longer tail than $N_r(E_B)$.

(ii) Instead of a single well-defined value there may be a distribution of threshold energies around a mean value. Such a distribution could be caused, first of all, by orientation effects.¹⁸ Secondly, atoms near structural defects, e.g., dislocations, may be bound less tightly than atoms on normal sites in the lattice. Thirdly, there is a 9% variation in the mass of stable Ge isotopes. Fourthly, at any finite temperature, thermal vibrations of the target atoms cause a "smearing out" of what began as a sharp threshold at absolute zero.

This last effect would cause a spread of $\pm 10\%$ around the mean at the temperature of our experiments,²¹ i.e., about 300°K. To take account of this fact, a recalculation of the number of recombination centers introduced into a sample was made, as indicated above, with the additional assumption that the probability of displacement is represented by a Gaussian distribution around a mean threshold energy $\langle E_{B0} \rangle$. A mean value of 425 kev was chosen for E_{B0} from an examination of the experimental data. The root-mean-square deviation of the Gaussian curve, ΔE , was fixed at 40 kev, i.e., approximately 10% of $\langle E_{B0} \rangle$. A set of $N_r(E_B)$ curves was then generated for values of E_{B0} around the mean. Each of this set [symbolized by $N_r(E_{B0}, E_B)$] was weighted by the probability that such a value of E_{B0} exists [symbolized by $w(E_{B0})$], and the resulting products were

²¹ The authors are indebted to J. W. Glenn who pointed out that if, in a collision, the struck atom acquires a velocity v_0 and if in addition it has a velocity due to thermal vibration of v_T , then the ratio of the minimum energy needed to displace an atom at temperature T to its value at $T=0$ is

$$(v_0 - v_T)^2 / v_0^2 \approx (1 - 2v_T/v_0) \approx 0.92 \text{ for } T = 300^\circ\text{K}.$$

See J. W. Glenn, Phil. Mag. Suppl. 4, 381 (1955).

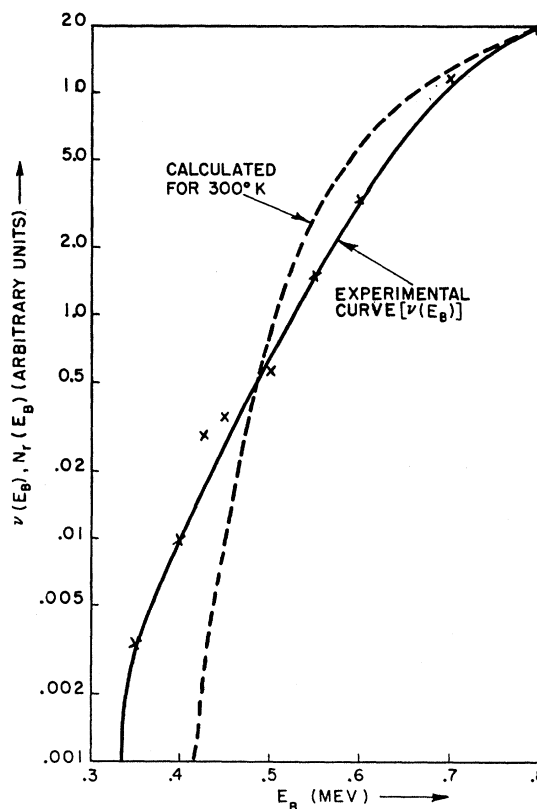


FIG. 12. Comparison between $\nu(E_B)$ and $N_r(E_B)_{300^\circ\text{K}}$.

summed for each value of the incident electron energy, E_B .²² A plot of $N_r(E_B)_{300^\circ\text{K}}$ versus E_B is compared to $\nu(E_B)$ in the linear plot of Fig. 11 and in the semilog plot of Fig. 12. The linear plot suggests that a displacement of about 20 kev would cause $N_r(E_B)_{300^\circ\text{K}}$ to coincide with $\nu(E_B)$ for energies in excess of say 525 kev. However, for lower energies the calculated curve predicts a smaller number of defects than what was found experimentally. This divergence is shown very clearly in the semilog plot of Fig. 12. It appears that the agreement between experiment and theory could be improved by using a value of ΔE larger than the 40 kev used in this calculation, which perhaps could be justified for the reasons already cited.

ACKNOWLEDGMENT

It is a pleasure to thank our colleague, Dr. F. D. Rosi, for permission to use his unpublished data.

²² In mathematical terms, the following quotient of sums was evaluated and identified with the number of recombination centers which will result if an electron beam of energy E_0 impinges on the sample at 300°K:

$$N_r(E_B)_{300^\circ\text{K}} = \frac{\sum_0^{E_B=800 \text{ kev}} N_r(E_{B0}, E_B) w(E_{B0}) \Delta E}{\sum_0^{E_B=800 \text{ kev}} N_r(E_{B0}, E_B) \Delta E}. \quad (a)$$

The quantity $w(E_{B0})$ has the following form:

$$w(E_{B0}) = (1/(2\pi)^{1/2} \Delta E) \exp[-((E_{B0}) - E_{B0})/2\Delta E]^2. \quad (b)$$